TWENTY FIRST EUROPEAN ROTORCRAFT FORUM

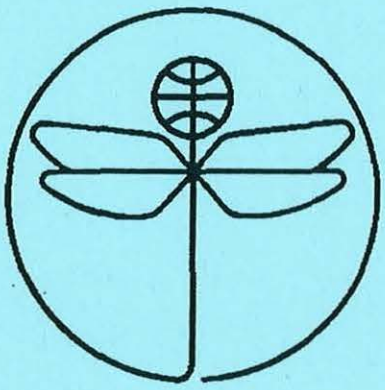

Paper No II.10

AN OPTIMIZATION METHOD APPLIED TO THE AERODYNAMICS OF HELICOPTER ROTOR BLADES

BY

Joelle Zibi

ONERA
FRANCE

August 30 - September 1, 1995

SAINT - PETERSBURG, RUSSIA

Paper nr.: II.10

An Optimization Method Applied to the Aerodynamics of Helicopter Rotor Blades.

J. Zibi

TWENTY FIRST EUROPEAN ROTORCRAFT FORUM
August 30 - September 1, 1995 Saint-Petersburg, Russia

AN OPTIMIZATION METHOD APPLIED TO THE AERODYNAMICS OF HELICOPTER ROTOR BLADES

Joëlle ZIBI

Office National d'Etudes et de Recherches Aérospatiales

BP72, 92322 Châtillon Cédex, France

Abstract

An aerodynamic optimization procedure has been developed for rotor blade design, and is applied to define optimum blade characteristics for a rotor in high-speed forward flight. For that purpose, the CONMIN optimizer was coupled to an aeroelastic helicopter rotor code R85 developed by Eurocopter France. The objective function is the minimization of the power consumed by the main rotor under constraints imposed on the pitch link loads. The first step consists in defining two optimized airfoils. Numerical results show significant improvements on the lift-to-drag ratio obtained from a good compromise between airfoils thickness and camber. The second step is to optimize the planform of an initial rotor, using the optimized airfoils described above. A first theoretical result recommends to increase the chord in the part of the blade where the airfoil lift-to-drag ratio is maximum. A swept tip is used to reduce the intensity of the shocks, and thereby the drag. However, the aeroelastic effects have to be considered very carefully for non rectangular blades.

1 - Introduction

The development of numerical methods applied to helicopter rotor aerodynamics leads to the design of new rotor blades. The design requires a large number of geometric and/or structural definition parameters, so that parametric studies are difficult to perform completely. The growing complexity of these rotors, and of their flight envelope are calling for more time-consuming computations. This is why numerical optimization methods have appeared to be an efficient design tool for rotor blades, as they provide better design compromises with less demand on human resources.

The flow around a helicopter blade is very complex. The main difficulties are the flow unsteadiness, the transonic conditions on the advancing blade, stall on the retreating side, and blade/vortex interaction. This explains why numerical optimization is not very advanced for three-dimensional aerodynamic configurations, because the aerodynamic computations in this case are relatively long and difficult to integrate into an optimization process. However, preliminary applications have been made for aircraft wings, by coupling a 3D solver with a numerical optimizer (Ref 1).

Also, the blade displacements and deformations depend on the flight configuration, and therefore have to be computed simultaneously as the aerodynamic equations. This explains why the optimization methods currently used for designing blades are based on relatively simple aerodynamic models, such as lifting line analysis, and are using 2D airfoil polars. Dynamic models, on the other hand, are more sophisticated as they are based on beam theory, with either a modal or finite element approximation (Ref 2). Nevertheless, aerodynamic models have been improved and validated through wind tunnel tests, in order to model advanced non rectangular rotor blades. NASA and US-Army have been working on a multidisciplinary programme on this topic (Ref 3). In France, a research programme on helicopter blade aerodynamic and dynamic optimization, called ORPHEE, has been developed between ONERA and ECF, with the financial support of the french Ministry of Defence (STPA). As simultaneous aerodynamic and dynamic optimization of a rotor blade is a very complex problem, it has to be considered separately to define two aerodynamically and dynamically (Ref 4,5) optimized rotors.

The purpose of this article is to present the computer tools used in the optimization process, then the determination of optimum airfoil characteristics for high speed forward flight, the first planform optimization process and finally

the first comparisons between experimental and R85 calculations results.

2 - Computer Tools

2-1 - Description of R85 Helicopter Rotor Code

The R85 aeroelastic rotor code developed by ECF (Ref 6) is an efficient tool for trimming the helicopter rotor and computing its performance for a given flight configuration. The code flowchart is given in Figure 1. The rotor is trimmed by solving the equations of mechanics iteratively for rotor blades under the effects of the aerodynamic and inertial forces.

The blade is modeled aerodynamically using the lifting line theory, in which the blade is discretized into a number of sections of which different aerodynamic coefficients are interpolated in files of 2D polar quasi-steady data. The wake effect is included either with a simple Meijer-Drees inflow model or with a vortex method (called METAR). A number of different computation options can be activated to simulate aerodynamic effects on non-rectangular blades (sweep, anhedral, transonic effects, etc).

From the dynamic point of view, we assume the blade to be either rigid or flexible. In the latter case, it is discretized spanwise in different segments, each of which is connected to the segments following it by three angles. The structural properties as the local blade section mass, stiffness and inertia are also a necessary input.

Different types of rotor trimming are available, using prescribed loads, prescribed commands, or a combination of the two.

2-2- Description of CONMIN optimizer

The CONMIN optimizer (Ref 7) is based on the feasible directions method. It consists in minimizing a non linear objective function within an admissible domain defined by constraints, which may be placed on the optimization variables themselves (lower and/or upper limits), but also on other terms derived from the previous rotor trimming process: pitch link loads, equivalent chord, etc.

The optimization process consists in computing the "best" search direction at a given iteration, to decrease the objective function most while satisfying all of the set constraints.

At a given CONMIN iteration q, the optimization process calls for about 1+ q(n+3) evaluations of the objective function (n being the number of optimization variables). This means that, in order to couple CONMIN with the R85 rotor code, this latter code must be robust and fast enough to avoid prohibitive computation times.

2-3 - Description of R85 - CONMIN coupling

The coupling flowchart is presented in Figure 2. For given rotor geometry and flight condition, the R85 code gives the pitch, flag and lag angles as well as the rotor loads and power provided by the rotor. These values are transmitted to the optimization subroutine through the objective function and the constraints. It should be said that we consider the Meijer-Drees model to find the induced velocities in the aerodynamic optimization process, for reasons of computation time, the METAR model being more realistic but also more time consuming.

3 - Aerodynamic optimization

The purpose of this optimization is to minimize the power consumed by the main rotor at a high-speed forward flight and realistic cruising flight lift (μ=0.463, C_T/σ=0.075). The design variables can be the spanwise evolutions of the chord, the twist angle, the quarter-chord line at the tip, the airfoil polars and their spanwise positions. The constraints are aerodynamic and geometric. The main one is a limitation on the maximum control force exerted on the pitch links.

In the ORPHEE operation, the first application of this aerodynamic optimization process is the definition of optimized airfoil polars which equip a rotor in high-speed forward flight (Ref 8). It can be noted that the blade is assumed to be rigid for the purpose of this process.

3-1 - Definition of Optimized Airfoils

A helicopter rotor blade is defined by five different airfoil sections at most, and each of these is defined by interpolation among at most

five polars. The optimization variables are the interpolation coefficients λ. The constraints applied to these variables are defined as :

$0 <= \lambda ij <= 1$; i=1,n and j=1,m(n)

in which n is the number of airfoil sections spanwise, and m(i) the number of polars defining the i^{th} section.

In the course of the optimization process, the new airfoil polars are interpolated in the polar files, which are defined on the basis of existing or extrapolated airfoil polars (Figure 3).

The basic idea is to allow a non-zero moment coefficient C_{m0} in order to obtain larger lifting capabilities and a better lift-to-drag ratio, while maintaining moderate pitch link loads by compensating the nose-down pitching moments existing on certain portions of the blade with nose-up pitching moments on other sections where a high C_{Lmax} is not required.

3-2 - Results of Airfoil Optimization

The optimization process is initialized by a modified 7A rotor configuration, called 7MB, with four rectangular blades. The OA312 airfoil is located from the root out to 85% of the radius, and the OA309 airfoil from 92% out to the tip.

A typical optimization case involves 10 optimization variables and requires about 10 CONMIN iterations. After optimization, the blade has three airfoil sections, but only two of them are optimized, since the R85 code cannot compute the blade tip precisely enough. This is why the OA309 airfoil is retained for the portion running from 95% of the radius out to the tip.

The optimized airfoil distribution is as follows (Figure 4):

- from 20% to 54% of the radius, airfoil section no.1 is used, with 11% relative thickness, and a nose-up pitching moment C_{m0}=0.044;

- optimized airfoil no.2, with 9% relative thickness, runs from 59% to 89% of the radius, at a nose-down pitching moment of C_{m0}=-0.02;

- the OA309 airfoil runs from 95% of the radius out to the tip. Its relative thickness is 9%, and its nose-up pitching moment is very low (C_{m0}=0.002)

It can be seen that the optimized rotor is thinner (i.e. in relative thickness) than the initial one. It also provides a power gain of 4.3% (Figure 5) around the optimization point (μ=0.45, C_T/σ=0.075). The performance is improved over the entire flight envelope, particularly at high velocity. However, thinning the blade tends to degrade its performance under high lift conditions, where stall occurs.

The pitch link load constraints are set at 300N for the static loads, and 600N for the dynamic. It can be seen on Figure 6 that, by combining a nose-up airfoil with a nose-down one, the control loads can be kept within allowable limits, while these constraints were violated at the optimization point for the initial rotor.

These optimum airfoil polars were used to define the technical specifications of a new generation of airfoils: the OA4 family.

3 3 - Analysis of results

To get a better understanding of where the power gains come from on the optimized rotor, we will compare three different rotors:

- the reference 7MB rotor;

- an "intermediate" rotor (Figure 4) for which only the OA312 and OA309 sections are optimized spanwise, to deal separately with the effects due to the thinning and to the camber of the airfoils;

- the optimized rotor.

Figure 7 compares the performance of the optimized airfoil 2, OA312 and OA309 airfoils. At transonic velocities (M=0.8), the lift of optimized airfoil 2 is improved without increasing the drag, which means a better L/D ratio. At low velocities (M=0.3), the C_{Lmax} of optimized airfoil section 2 is very close to that of the OA312 airfoil.

Figure 8 shows the drag variation at 89% radius (corresponding to the end position of optimized airfoil 2) at the optimization point for the three rotors studied. By thinning the optimized and intermediate rotors, the drag divergence due to the transonic effects can be moved back

on the blade, which greatly reduces the drag (in particular on the advancing blade) and therefore the rotor power requirement.

For a flight configuration closer to stall (C_T/σ=0.09), the lift force distribution along the blade at azimuth ψ=300° (Figure 9) shows the major role played by optimized airfoil 2. That is, at 90% of the radius, the optimized airfoil 2 delays the occurence of stall thanks to its negative moment coefficient, which improves its lift capabilities, while the intermediate rotor has already stalled at the same radius, under effects of the OA309 airfoil. So the loss in maximum lift due to the thinning of the optimized blade is compensated by the camber law of optimized airfoil 2, whose C_{Lmax} capacities are comparable to those of the OA312 with the 12% relative thickness.

4 - First Planform Optimization

The first step in the aerodynamic optimization process was therefore to define two optimized airfoils: one is a nose-up airfoil with 11% relative thickness, and the other is a nose-down airfoil with 9% relative thickness.

The second step consists in optimizing the planform and twist of an initial blade using optimized airfoils 1 and 2. Helicopter rotor blade planform optimization to date have concerned only the blade tip, ie the last 5% of the radius. Furthermore, the lifting line theory is less accurate for these complex configurations, so are the calculations of the gradients.

The potential benefits of a planform optimization are searched in two directions:

- on the one hand, the blade tapering, which tends to concentrate the surface of the blade in the useful areas;

- on the other hand, the sweeping of the blade tip, which allows a stall delay on the retreating side of the blade.

As before, the optimization point is set at μ=0.463 and C_T/σ=0.075.

It can be noted that during the optimization process, the blade is supposed to be rigid for reason of CPU time. But, the aeroelastic effects induced by the aerodynamic and dynamic effects can play a very important role for non rectangular blades. That is the reason why the behaviour of the blade issued from the "rigid" optimization process has to be checked by R85 calculations using the flexible model.

A first "theoretical" result is obtained by this complex process, giving a highly non-rectangular blade. For that case, the dynamic effects have to be considered very carefully in cooperation with IMFL which is in charge of the technological definition of the blade (Ref 9). In addition to the two airfoil polars mentioned above, this blade includes a thick airfoil section at the root to improve the stiffness of the blade and to compensate the torsional moments induced by the swept tip (Figure 10). Furthermore, a thin airfoil section at the tip is used to reduce the intensity of the shocks, and thereby the drag and noise.

Moreover, the chord is increasing in the part of the blade where the lift-to-drag ratio of the airfoil is maximum, in order to concentrate all the efforts in these aeras. In that way, the rotor can be made to operate at a higher lift.

Lastly, sweeping back the tip allows a better behaviour of the rotor at high-speed forward flight. Concerning the twist, the optimization process yielded no significant change compared to the initial blade.

5 - First experimental results

A first planform optimization was performed. The next step consists in improving this optimized configuration and then, to define, design and construct the aerodynamically optimized rotor blade wind tunnel model, in order to check that the theoretical mechanical and mass characteristics determined during the optimization process are technologically possible.

The wind tunnel tests were performed in the ONERA S1 wind tunnel in Modane, with its 8-meter-wide test section. The rotor is installed on a special test rig and is driven electrically, with hydraulic trim controls to follow an arbitrary control law. The test configurations were chosen to be representative of the entire flight envelope, the nominal optimization point being μ=0.463 and C_T/σ=0.075.

It can be reminded that the objective of the optimization process is to minimize the power consumed by the optimized rotor with respect to a reference rotor. For the nominal optimization advance ratio (μ=0.463) and for the control law called "Modane" law used in the wind tunnel, for which β_{1S}=0 and β_{1C}=-θ_{1S}, Figure 11 shows the relative difference in terms of power consumed by the optimized rotor between calculation and experiment for two flight configurations (C_T/σ=0.075 and C_T/σ=0.1 close to stall). A very good correlation between the experiment and R85 calculations is found, the difference being less than 1%. Furthermore, at the nominal optimization point, the difference between the experimental and theoretical power benefits between the optimized rotor and the reference rotor is equal to 0.8%. Of course, this validation has to be continued over the entire flight envelope, but these results show that the R85 code can correctly predict performance for highly non rectangular rotor blades.

On the other hand, it is interesting to account for the aeroelastic behaviour of the optimized rotor, including the torsional, flapping and lag deflections. For that purpose, the blade is supposed to be flexible, and the METAR wake model is used, in order to obtain realistic soft blade simulation. At the nominal optimization point, and for the so-called "Modane" control law, Figure 12 shows the difference between the calculated peak-to-peak flapping, lag, torsional moments, and the pitch link loads, with respect to the experimental values. We can deduce from these results that these moments and loads amplitude are quite well predicted. Furthermore, it can be noted that, since the pitch link loads were constrained during the optimization process, they remained below a reasonable value during the wind-tunnel tests. This shows that the R85 rotor code can correctly take into account the anhedral and the swept tip influence on the optimized blade dynamics.

6 - Conclusions and future evolutions

A numerical helicopter blade optimization process has been developed at ONERA, in cooperation with Eurocopter France, under the ORPHEE programme. This process uses a helicopter rotor trimming code (R85) coupled with an optimizer (CONMIN) and was used to improve the aerodynamics characteristics of a reference rotor.

From the aerodynamic optimization, a new family of airfoils was first defined (the OA4 generation) and allowed an optimum spanwise airfoil distribution. This led to a power gain of 4.3% for high-speed forward flight. The new rotor also offers power gains over a broad flight envelope, compared to a reference rotor.

Then, the next step was to design a new planform, and to construct the rotor blade wind tunnel model for the ONERA S1 wind tunnel in Modane. The correlations between the experimental and calculated performance of the optimized rotor, for high-speed flight (μ=0.463) are very good, and the power benefit at the optimization point is very close to the predicted one.

These results show the effectiveness of the optimization process in improving aerodynamic rotor properties. The next step will be to apply the dynamic optimization process in order to define a globally optimized rotor, ie one that is optimized aerodynamically and dynamically.

7 - References

1 . D. Destarac, J. Reneaux and D. Gisquet. Numerical Optimization of Wings in Transonic Flows. Agard Conference, Norway, May 1989.

2 . J.W. Lim and I. Chopra. Aeroelastic Optimization of a Helicopter Rotor. 44th AHS Forum, Washington D.C., June 1988.

3 . H.M. Adelman, W.R. Mantay, J.L. Walsh and J.J. Pritchard. Integrated Multidisciplinary Rotorcraft Optimization Research at the NASA Langley Research Center. Vertiflite, March-April 1992, Vol.38, No.2.

4 . J. Zibi, P. Leconte and P. Geoffroy. Helicopter Rotor Aerodynamic and Dynamic Optimization Methods. La Recherche Aerospatiale, 1995, No. 3.

5 . P. Leconte and P. Geoffroy. Dynamic Optimization of a Rotor Blade. AHS Aeromechanics Specialists Conference, San Francisco, 1994.

6 . M. Allongue and T. Krysinsky. Validation of a New General Aerospatiale Aeroelastic Rotor Model through the Wind Tunnel and Flight Test Data. 46th AHS Forum, Washington D.C., May 1990.

7 . G.N. Vanderplaats. A Fortran Program for Constrained Function Minimization. NASA TMX62282, 1973.

8 . J. Zibi, G. Desfresne and M. Costes. A Numerical Procedure for Aerodynamic Optimization of Helicopter Rotor Blades. 18th ERF, Avignon, September 1992.

9 . F. Dupriez, P. Geoffroy and B. Paluch. Design and Manufacturing of Torsional Flexible Blade Models. 16th ERF, Glasgow, 1990.

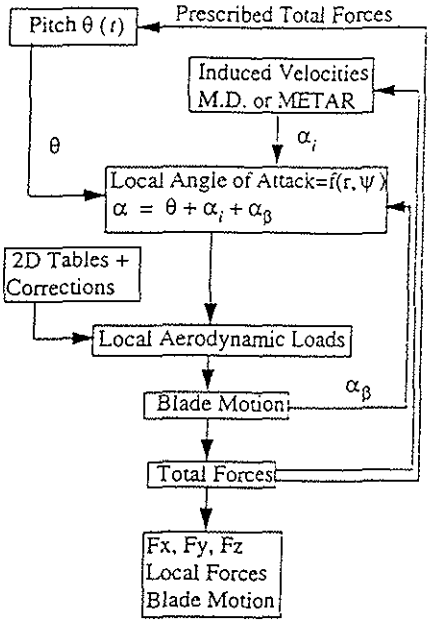

Figure 1 : R85 flowchart

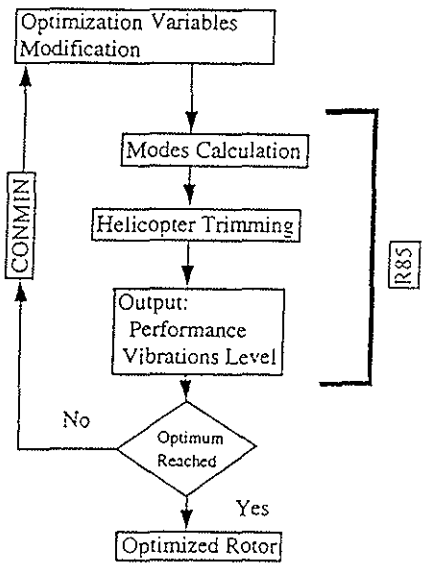

Figure 2 : Coupling R85/CONMIN flowchart

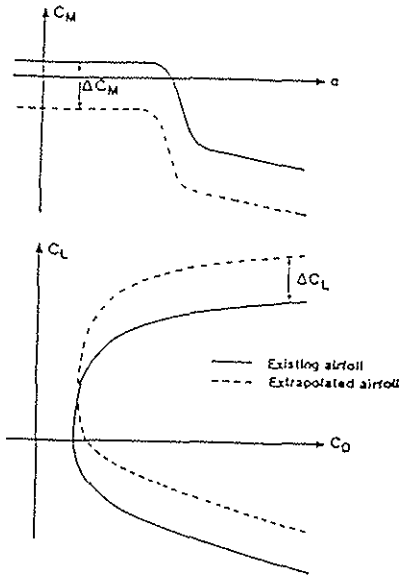

Figure 3 : Definition of extrapolated airfoil polars

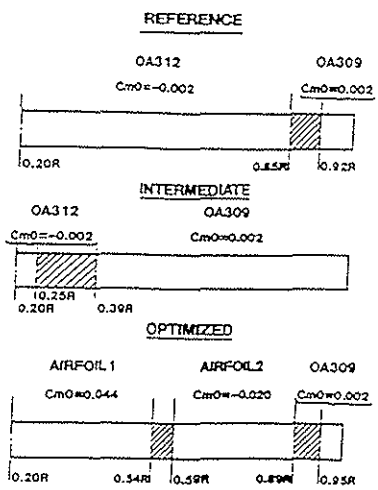

Figure 4 : Airfoil optimization for high speed flight

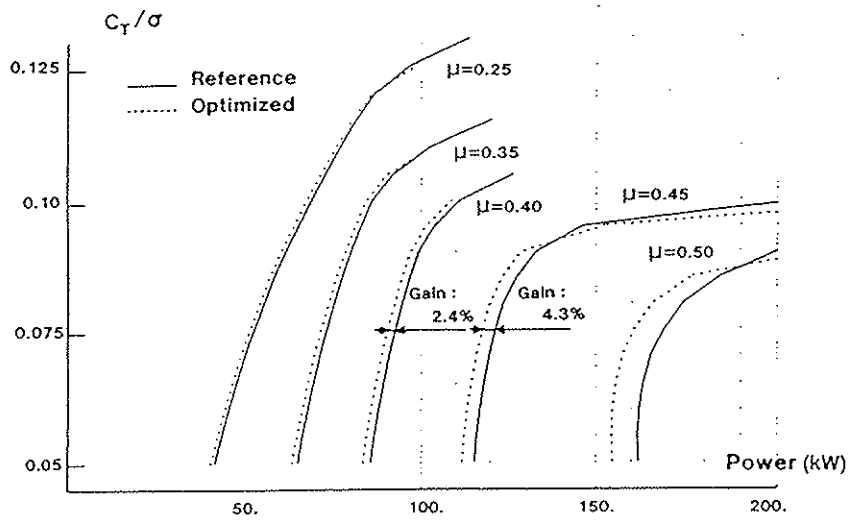

Figure 5 : Comparison of the flight envelope

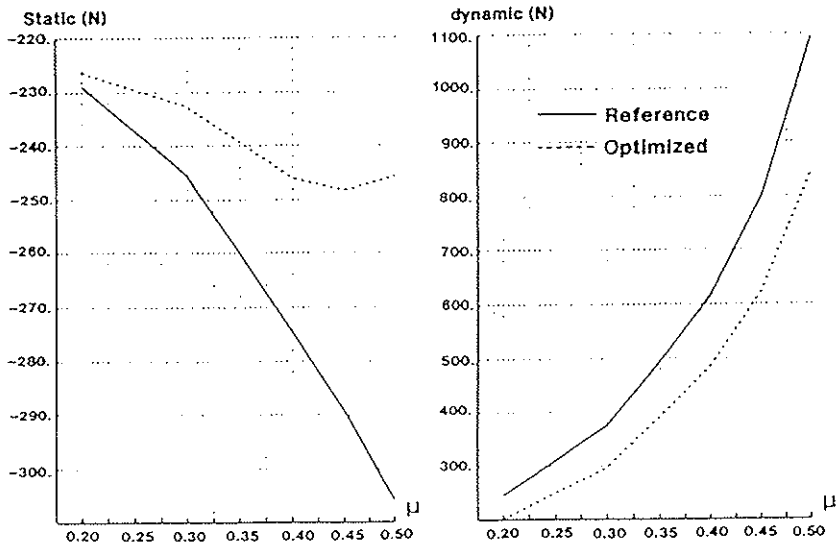

Figure 6 : Comparison of the pitch link loads

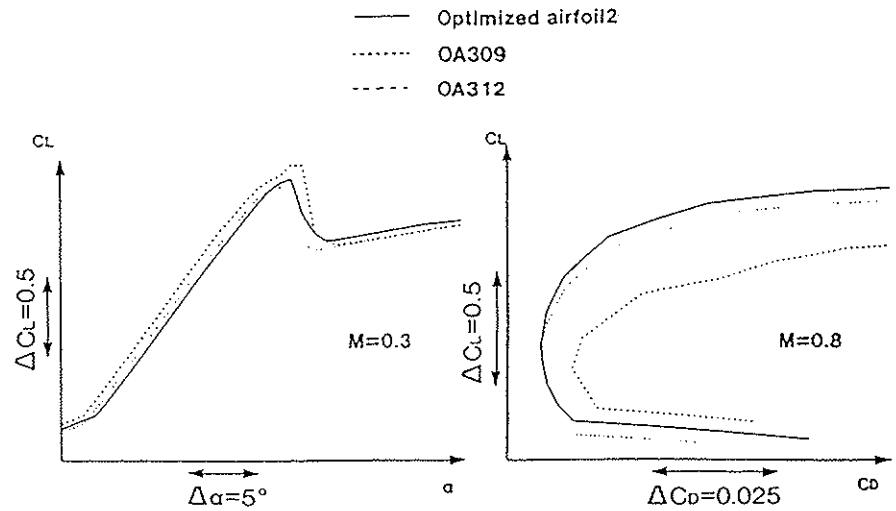

Figure 7 : Performance of the OA309, OA312 and no.2 optimized airfoils

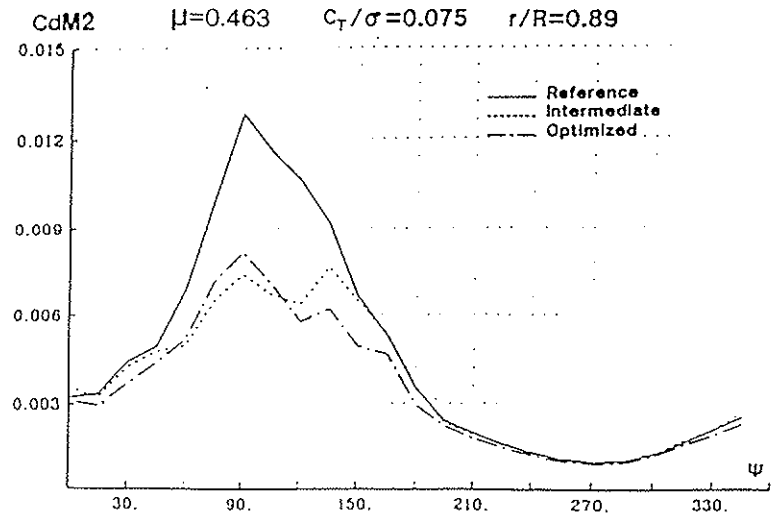

Figure 8 : Comparison of the drag evolution

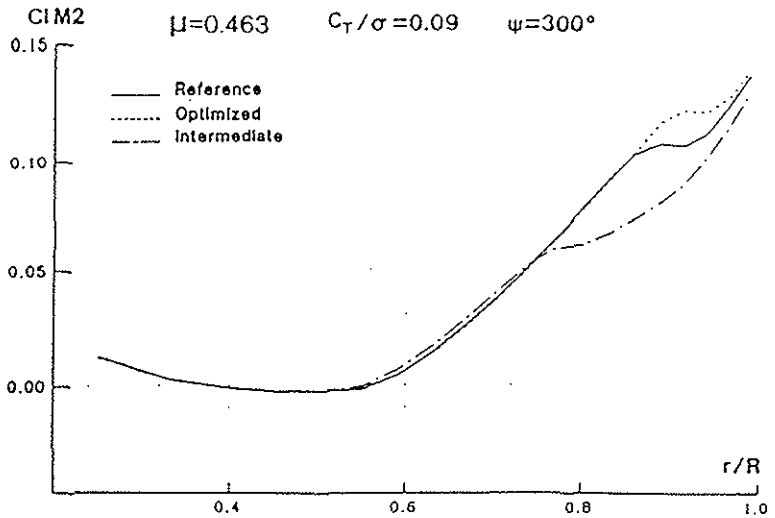

Figure 9 : Comparison of the lift evolution

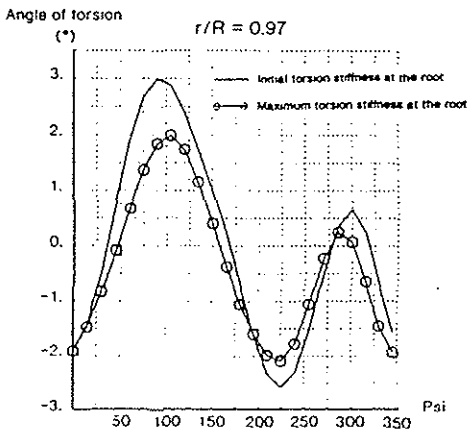

Figure 10 : Torsional deformations

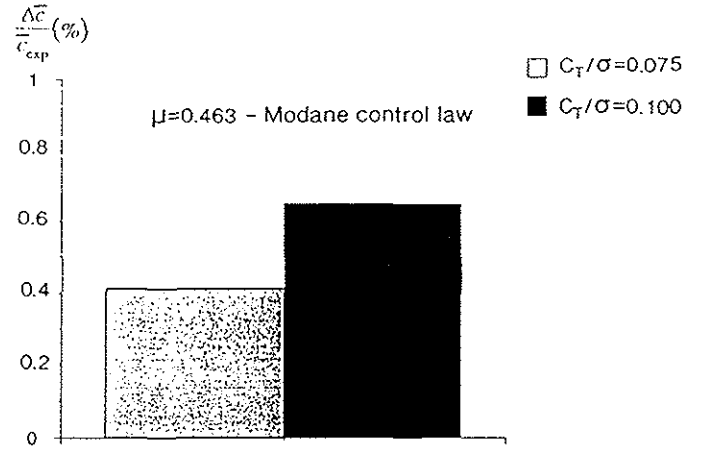

Figure 11 : Difference between calculated power with respect to the experiment

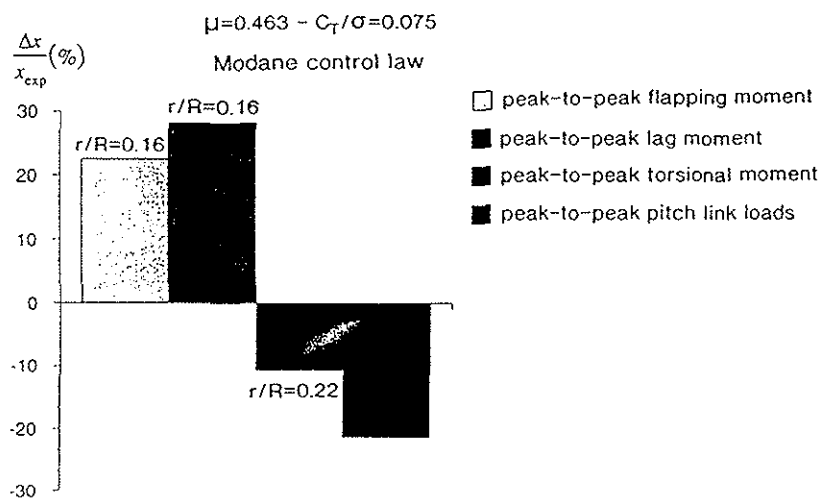

Figure 12 : Difference between the calculated peak-to-peak moments and pitch link loads with respect to the experiment